ATOMIC PROCESSES IN ASTROPHYSICS

JOHN C. RAYMOND and NANCY S. BRICKHOUSE
Harvard-Smithsonian Center for Astrophysics, 60 Garden Street, Cambridge, MA 02138, USA

Abstract.
We review the atomic processes responsible for astrophysical emission line spectra, paying particular attention to the reliability of the rates used to determine the physical conditions in the emitting gas. We discuss particular cases where often-neglected processes play important roles.

1. Introduction

The spectrum of an astrophysically interesting object can, at least in principle, be reduced to an unambiguous set of emission line intensities, continuum fluxes, and absorption line profiles. This reduction is generally limited by blending (especially at the low to moderate spectral resolution of most EUV and X-ray instruments), by uncertainty in the intensity calibration (up to 30%, though relative intensities at closely-spaced wavelengths may be more reliable), or "irrelevant" complications such as uncertain interstellar attenuation.

Given a measured spectrum, one wishes to derive the temperature distribution, density, ionization state and elemental composition of the observed plasma. An enormous number of atomic rates is needed to interpret the spectra of celestial objects in terms of physical parameters. Recent reviews of theoretical emission spectra include Raymond (1988) and Mewe (1991) concentrating on X-ray spectra, and Brickhouse, Raymond, and Smith (1995) and Mason and Monsignori-Fossi (1994) concentrating on the EUV. Critical reviews of atomic rates include the collision strength bibliography of Pradhan and Gallagher (1992), an issue of "Atomic Data and Nuclear Data Tables" (Vol. 57, Nos. 1/2, 1994) devoted to collision rates, the ionization rate study of Kato, Masai, and Arnaud (1991), The Opacity Project book just published by The Institute of Physics Publishing and the review of nebular emission line data of Pradhan and Peng (1995).

The above reviews are reasonably comprehensive, and progress has not been so rapid that they are entirely out of date. Therefore, we will try to complement these works by giving a brief overview of which rates are most important in common applications. We also give some opinions as to the typical level of uncertainty in the rates. These are based partly on the degree of consistency among measured or computed cross sections and partly on the scatter obtained when one attempts to fit $\sim$ 100 lines at once (Brickhouse *et al.* 1995). It is also important to maintain a healthy skepticism toward generalizations about which processes are important. The

Astrophysics and Space Science **237**: 321–340, 1996.

Universe is large enough that even the most obscure process is probably important somewhere. Therefore, we give examples of some of the lesser-known correction terms which can dominate in unusual circumstances.

We close this introduction with a brief harangue. One approach to the bewildering amount of information in a high quality spectrum is to choose one or two lines from which to derive one physical quantity, such as N_e, T_e, or an elemental abundance ratio. This approach has the considerable advantage that one can choose lines which are bright and easy to measure, and for which reliable atomic data are available. Its disadvantages are also considerable. Astrophysical plasmas are seldom isothermal or isochoric. Also, someone who selects a single diagnostic ignores a great deal of information obtained at great expense and may obtain results which are inconsistent with the intensities of other lines in the spectrum. And finally, our opinions as to which atomic rates are most reliable have frequently proven incorrect. Therefore, we believe it to be more profitable to fit a large number of lines at once. This provides a sobering perspective as to the reliability of both the observations and the theory, and it provides a feeling for the range of conditions within the object observed.

2. Basic Assumptions of Plasma Emission Models

2.1. Level Population Calculations

The radiative decay of an excited state of an atom or ion produces an emission line whose intensity depends on the population of the excited level and on the Einstein transition probability A_{kj} from upper level k to lower level j. For an optically thin plasma, all emitted photons "escape" and thus the radiated power per volume, or volume emissivity ε, is given by

$$\varepsilon = \frac{hc}{\lambda} N_k A_{kj}, \tag{1}$$

with ε in ergs cm^{-3} s^{-1} and N_k the level population density. For small optical depths (of order a few) Equation 1 may be modified by a photon escape probability factor, which depends on the scattering geometry. For larger optical depths, the assumptions of our model break down, and a full radiative transfer model is required.

The population density of level k is in general a function of time, which includes all processes that populate and depopulate the level.

$$\frac{dN_k}{dt} = \sum_i N_i R_{ik} - N_k \sum_i R_{ki} + N_k F_k, \tag{2}$$

where the rates R_{ik} and R_{ki} in s^{-1} are summed over all possible energy levels i. F_k is the net flux of ions in excited state k into (or out of) the emitting

region by advection or diffusion processes. In this section we assume $F_k = 0$, and focus on the atomic rates that contribute to line emission.

Under conditions of statistical equilibrium the level populations are constant with time, and are found by the simultaneous solution of the rate equations for all energy levels. With a model of time-dependent heating or cooling, non-equilibrium problems may be solved as well, although models may be less constrained as more free parameters become available. We discuss some examples in the next section. The most general treatment of transition rates involves the computation of transitions between all levels, including transitions between levels of different ionization stages. The rate from any level m to any other level n is then given by

$$R_{mn} = R_{ioniz} + R_{recomb} + \sum_s N_s q_{s,cx} + A_{rad} \qquad + \sum_s N_s q_{s,coll}, \qquad (3)$$

where R_{ioniz} is the sum of photoionization and collisional impact ionization rates, R_{recomb} is the sum of radiative, dielectronic, and 3-body recombination rates, and the charge exchange rate is the sum of the individual charge exchange rates, where $q_{s,cx}$ are the rate coefficients and N_s is the population density of the interacting species. A_{rad} includes stimulated absorption (photo-excitation) as well as spontaneous radiative decay, and the collisional rate includes collisional excitation and de-excitation processes, with $q_{s,coll}$ the collisional rate coefficient for interaction with species s. In detail the rate from lower level j to upper level k is given by

$$R_{jk} = N_e q_{ioniz} + \overline{S}\beta_{photoioniz} + N_p q_{cxioniz} + \overline{J}B_{jk} + N_e q_{e,ex} + N_p q_{p,ex}, \qquad (4)$$

where $\overline{J}$ and $\overline{S}$ are radiative source terms for photoexcitation and photoionization, respectively. The collisional excitation processes are generally dominated by electron collisions, but protons or other species may also be important. The collision rates are proportional to the densities of the impact species through N_e and N_p. The rate coefficients q_{ioniz} for electron impact ionization from level j to level k, $q_{e,ex}$ for electron impact excitation, $q_{p,ex}$ for proton impact excitation, and $q_{p,cxioniz}$ for charge exchange have units of $\mathrm{cm}^3\ \mathrm{s}^{-1}$.

$$B_{jk} = \frac{g_k}{g_j}\frac{\lambda^3}{2hc}A_{kj}, \qquad (5)$$

where g_k/g_j is the ratio of the statistical weights. For a similar level of detail, the depopulation rate from level k to level j is given by

$$R_{kj} = N_e\alpha_{rad} + N_e\alpha_{di} + N_e^2\alpha_{3-body} \quad + N_{\mathrm{H}^0}\, q_{cxrecomb} + A_{kj} \\ + N_e q_{e,de-ex} + N_p q_{p,de-ex}, \qquad (6)$$

where α_{rad}, α_{di}, and α_{3-body} are the radiative, dielectronic, and three-body recombination rate coefficients, respectively. The rate coefficients $q_{e,de-ex}$

for electron impact excitation, $q_{p,de-ex}$ for proton impact excitation, and $q_{cxrecomb}$ for charge exchange have units of cm^3 s^{-1}. By the principle of detailed balancing, the three-body recombination is the inverse of electron impact ionization, and thus

$$\alpha_{3-body} = \frac{1}{2}\frac{h^3}{(2\pi mkT_e)^{\frac{3}{2}}}\frac{g_j}{g_k}\exp(\frac{\triangle E}{kT_e})q_{ioniz}, \tag{7}$$

where α_{3-body} has units of cm^6 s^{-1}. Similarly, $q_{cxrecomb}$ is the inverse of $q_{cxioniz}$. With typical astrophysical abundances, charge exchange with neutral hydrogen (H°) is the most important charge exchange recombination process. Through detailed balance q_{de-ex} is related to q_{ex},

$$q_{de-ex} = \frac{g_j}{g_k}\exp(\frac{\triangle E}{kT_e})q_{ex}, \tag{8}$$

where $\triangle E$ is the energy difference between levels j and k and T_e is the electron temperature.

The rate equations for all levels of all ionization stages may be solved simultaneously in the steady-state approximation for a given T_e, N_e, and, where collisions with hydrogen are important, N_H/N_e. Double ionization and recombination processes are relatively rare, and are ignored here, although K-shell ionization followed by Auger ionization may be significant in rapidly ionizing plasmas, such as young supernova remnants. The general case outlined here is in practice made more tractable by imposing a number of simplifying assumptions. Solving for the ionization balance may be decoupled from the line excitation problem for the low density case in which most of the ion population resides in the ground state level. First the population density of a given ionization stage is determined, then the level populations for that ion may be computed, including ionization and recombination population processes. At higher densities, the population of metastable levels and fine-structure levels within the ground state may build up substantially. For example, one might need to include a collisionally excited metastable level in the ionization balance if collisional ionization from that level is important.

The statistical equilibrium problem may also be simplified by lumping together energy levels. Two examples are the treatment of collisional ionization from subshells and the treatment of excitation and decay for multiplets (statistically weighted averages of transitions between fine-structure levels). In practice, the number of energy levels n included in the model ion is limited by the program's goals. Above some critical n collisional processes are much more important than radiative processes, and the level populations are determined by their statistical weights. The number of levels can be limited much further if the levels that emit observable lines are populated only by collisional excitations and not by radiative cascades from the decay of higher levels.

Sobelman, Vainshtein, and Yukov (1981) describe three basic types of plasma emission models: coronal, collisional-radiative (CR), and local thermodynamic equilbrium (LTE). The electron density and optical depth essentially determine the range of applicability of these models. For very high densities (LTE) or optical depths the calculation of level populations is greatly simplified since collisions dominate. At intermediate densities ($N_e \sim 10^{12} - 10^{18}$ cm^{-3}), the most stringent requirements are placed on the formulation of the CR (or non-LTE) model ion and on the coupling of ionization balance and level population. At very low densities, the problem again is simplified, as most of the population of an ion exists in the ground state, so only ground state levels determine the ionization balance. In the coronal model, heating balances the radiative power loss, and the heating mechanism need not be specified for a unique temperature determination. For many high energy astrophysical sources, photoionization by an extremely hot source may dominate the ionization of surrounding gas. For these cases the nebular approximation is analogous to the coronal case, in that most of the population of the ions is found in the ground state (cf. Osterbrock 1974). Again, for moderately high densities, such as might be expected in low mass X-ray binaries ($\sim 10^{13}$ cm^{-3}), a full CR model is necessary (Liedahl *et al.* 1990, 1992). In the nebular model the photoionizing source is often the dominant heating source, and thus heating and ionization state are coupled. Kahn and Liedahl (1995) review X-ray spectroscopy with comparisons of coronal and photoionized sources.

The coronal equilibrium model then separates into two independent sets of equations:

$$N_z N_e(\alpha_{rad,z} + \alpha_{di,z}) + N_z N_e q_{ioniz,z} = N_{z-1} N_e q_{ioniz,z-1} + N_{z+1} N_e(\alpha_{rad,z+1} + \alpha_{di,z+1}), \quad (9)$$

for the ionization balance, and

$$N_k N_e \sum_l q_{e,kl} + N_k \sum_j A_{kj} = \sum_l N_l A_{lk} + N_e \sum_j N_j q_{e,jk}, \quad (10)$$

for the level populations. In the very low density coronal model, and for a resonance line which decays only to the ground, the coupled level population equations reduce to the simple formulation

$$N_k A_{kg} = N_g N_e q_{e,gk}, \quad (11)$$

where g denotes the ground state. With the line emissivity given by Equation 1, coupled level population calculations are then unnecessary to produce the spectrum of strong resonance lines. On the other hand, electron densities in the solar corona, for which the coronal model is named, are not sufficiently low to ignore collisional de-excitation for multiplet ground states and low-lying metastable levels. Even strong resonance lines such as Fe IX λ171.03

may be affected by the depopulation of the ground state at active region densities ($> 10^9$ cm^{-3}). Furthermore, for metastable levels of certain coronal ions, such as the $3p^3\ ^2P_{3/2}$ excitation of [Fe XII] λ1242, cascades from upper levels can contribute more than half of the level population. We prefer to calculate the full set of transitions in order to solve as accurately as possible for useful N_e and T_e diagnostic lines.

2.2. Atomic Rate Coefficients

The rate coefficients given in these equations are of general importance and we discuss these rate coefficients in some detail now. Fitting formulas which are useful for calculating rates can be found in the many review articles listed in the Introduction. We concentrate here on the rates of dominant processes.

We expect the radiative rate coefficients to be fairly accurate for strong transitions. Radiative recombination is the inverse of photoionization, and thus related to the photoionization cross sections by detailed balance. Photoionization cross sections in the threshold region for ions of astrophysical interest are recently available as part of the Opacity Project (1995), and continue to be updated. The extrapolation to high energy of Verner and Yakovlev (1994) includes the partial photoionization cross sections for subshells (Verner *et al.* 1993). These data represent a great improvement over the last few years. Thus the accuracy might be expected to be 10%.

As mentioned above, the strong resonance lines in coronal models do not even depend on the radiative transition probabilities. While transition probabilities, or A-values, for these lines are probably accurate to a few percent, the intersystem and forbidden line A-values may be much less accurate. An example is C III] λ1909 for which theoretical rates agree with each other to better than 10%, but the laboratory measurement is discrepant with some of the calculations by 20% (Kwong *et al.* 1993). For multi-electron ions of high Z elements, the theoretical values may disagree by 25% or more, as in the case of the well-known coronal green line, [Fe XIV] λ5303 (Bhatia and Kastner 1993; Huang 1986; Froese-Fischer and Liu 1986). Since line ratio diagnostics for N_e ultimately derive from the trade-off between collisional de-excitation and radiative decay, relatively large uncertainties are possible in the derived densities. Furthermore, line ratios of coronal forbidden lines, which are used as temperature diagnostics, are also subject to inaccuracies of the A-values (*cf.* Esser *et al.* 1995).

Under equilibrium conditions, electron collisional rate coefficients are averages of the cross section over the electron velocity distribution. This velocity distribution f(E) is usually taken to be Maxwellian, such that,

$$f(E)dE = \frac{2}{\sqrt{\pi}} \left(\frac{E}{kT}\right)^{3/2} \frac{e^{(-E/kT)}}{\sqrt{E}} dE. \tag{12}$$

When collisions with protons are important, the proton velocity distribution may also be assumed Maxwellian, even without equal proton and electron temperatures. Since collisional processes dominate in coronal plasmas, the uncertainties in their calculated values tend to dominate the errors. Very few laboratory measurements have been made, and many assessments of accuracy are based on the relative convergence of different theoretical approaches.

Direct collisional ionization rate coefficients may be calculated as a sum over the subshells of the ionizing ion, with each term in the sum proportional to a Boltzmann factor $e^{-\triangle E/kT}$, where $\triangle E$ is the energy difference between the subshell and the ground state of the ionized ion. For highly stripped ions an additional ionization process, excitation-autoionization, is important. Here an inner subshell electron is collisionally excited to a bound state above the ionization threshold, and subsequently autoionizes. (Autoionization is also called Auger ionization. An alternative decay path for this unstable bound state is the radiative decay process called excitation fluorescence.) Experimental measurements such as those of Gregory *et al.* (1986, 1987) confirm both direct and excitation-autoionization contributions. The typical uncertainties are probably about 20%. The situation is better for ions studies with crossed beams, and worse for very complicated ions.

Dielectronic recombination generally dominates recombination for coronal plasmas. The exceptions are very cool plasmas and ions which have no low-lying excited states: bare nuclei, H-like, He-like and Ne-like ions. The process involves formation of a doubly excited level, followed by radiative decay of the captured electron. The incoming electron has an energy below the threshold for the collisional excitation, and thus is captured into a highly unstable level above the ionization threshold of the recombined ion. This electron can either autoionize, or it can radiatively decay. The radiative decay process leads to the recombination. The photons emitted contribute to dielectronic satellite lines in the emission line spectrum. While the satellite lines are important diagnostics for X-ray spectra, they are usually weak relative to the collisionally excited lines. Among the complications of calculating dielectronic recombination rate coefficients are the need for very large numbers of energy levels (several hundred for some cases) and the calculation of accurate autoionization rates for doubly excited levels. For high n, LS coupling breaks down. Furthermore, the experimental verification of dielectronic recombination cross sections is limited (*e.g.* Story, Lyons, and Gallagher 1995). For H-like and He-like ions, as well as for most low to moderate Z ions, the uncertainties may be about 20%, but discrepancies as large as factors of two exist between different theoretical calculations (*cf.* Arnaud and Raymond 1992).

The effective collisional excitation rate coefficient (i.e. the Maxwellian integral $q_{e,ex}$) depends on the product of $\frac{1}{\sqrt{T}}e^{-\triangle E/kT}$ and the collision

strength Ω_{jk}. At high temperature (relative to $\triangle E$), Ω_{jk} is a slowly varying function of energy; however, for energies near threshold, the colliding electron may be captured during the excitation process as described for dielectronic recombination. When autoionization occurs, rather than photon emission leading to recombination, the resonant process can dramatically increase Ω_{jk} at that energy. Thus Ω_{jk} may have a complicated structure due to resonances near threshold. The net effect in the Maxwellian average is to increase the effective collision strength particularly for forbidden or intersystem transitions. Collision strengths may be as accurate as 10% if resonances are properly treated, as in close coupling calculations (*e.g.* Callaway 1994). In distorted wave approximations resonances are ignored and results are generally accurate to only about 30%. If the electron temperature is low, the Maxwellian average is more heavily weighted by the resonant structure and the accuracy decreases accordingly. Furthermore, ignoring resonances systematically affects the very line ratios (forbidden-to-allowed) that are used for electron density diagnostics. For the complex multi-electron ions, we believe factor of two errors in $\triangle n = 0$ transition lines are likely to remain; as $\triangle n$ increases, the simple approximations (*e.g.* Gaunt factor) still in use in astrophysics become increasingly less accurate. Factor of five errors have been suggested for $\triangle n = 2$ transitions of highly ionized Fe around 1.0 keV (Liedahl, Osterheld, and Goldstein 1995). More accurate calculations for X-ray and EUV lines are a high priority.

2.3. Spectral Emission

Once the level populations are calculated the line emission is given, in units of ergs cm^3 s^{-1}, by

$$P_\lambda = \frac{\varepsilon}{N_e N_H} \tag{13}$$

It is necessary to relate the level population N_k to the given quantity in the model N_e, where

$$N_k = \left(\frac{N_k}{N_z}\right)\left(\frac{N_z}{N_Z}\right)\left(\frac{N_Z}{N_H}\right)\left(\frac{N_H}{N_e}\right) N_e, \tag{14}$$

and $\frac{N_k}{N_z}$ is the solution of the level population equations for level k relative to the entire population of that ionization stage z; $\frac{N_z}{N_Z}$ is the population of z relative the population of element Z, derived from the ionization balance; $\frac{N_Z}{N_H}$ is the element abundance relative to hydrogen; and $\frac{N_H}{N_e}$ is about 0.8 for fully ionized gas of cosmic abundance. A standard set of solar elemental abundances is very widely assumed for interpreting low spectral resolution observations, but abundances in the solar corona are observed to vary by

factors of 3, so this assumption is dangerous. The intensity of a line observed at the Earth, from a source at distance r, in units of ergs cm^{-2} s^{-1}, is then

$$I_{Earth} = \frac{P_\lambda}{4\pi r^2} \int N_e N_H dV. \tag{15}$$

The integral $\int N_e N_H dV$ is the emission measure, generally taken over a specified temperature interval.

Spectral observations which yield a large number of high signal-to-noise, unblended lines from a range of temperatures offer the opportunity to construct emission measure distributions and thus utilize the wealth of spectral information on densities, abundances, and other parameters in the context of the temperatures of line formation. Until recently, few non-solar moderate resolution spectra for temperatures above $\sim 10^6$ K existed. Since the launch of the *EUVE* satellite in 1992, a number of high quality spectra have been obtained for stellar coronae, and analysis based on emission measure modeling is yielding insights into the conditions of these sources. While the spectral resolution is modest, and line blending compromises the interpretation for some lines, the flux calibration is remarkable ($\sim$ 15%). Fig. 1 shows three sample spectra, chosen for their different dominant temperatures, obvious from their strong spectral lines: Capella ($\sim 10^7$ K, based on Fe XVIII–XXIII), Procyon ($\sim 10^6$ K, based on Fe IX–XIV), and Epsilon Eri ($\sim 4 \times 10^6$ K, based on strong Fe XV and XVI). Analysis based on emission measure distribution modeling of strong lines for these sources may be found in Dupree *et al.* (1993), Brickhouse *et al.* (1995), and Brickhouse (1995) for Capella, in Drake, Laming, and Widing (1995) for Procyon, and Laming, Drake, and Widing (1995) and Schmitt *et al.* (1995b) for Epsilon Eri.

As an example of modeling a large number of emission lines, we present in Fig. 2 models of the emission measure distribution for a solar active region (Brickhouse *et al.* 1995). Other such analyses may be found in Raymond (1988) and Lang, Mason, and McWhirter (1990). The intensities for nearly 100 emission lines of iron over several ionization stages (Fe IX–XVII) are taken from the Solar EUV Rocket Telescope and Spectrograph (*SERTS*) active region catalogue of Thomas and Neupert (1994). Several branching ratio pairs are found in this set of lines, and the agreement for all but a few is within the expected range. The models compare the ionization balance of Arnaud and Rothenflug (1985) and Arnaud and Raymond (1992). Each line emissivity is integrated over the entire emission measure distribution, and the fit is achieved iteratively. The emission measure distribution is given in steps of 0.1 dex in T_e (K). The comparison between observed and predicted lines in Fig. 3 is for the newer ionization balance, but the agreement is comparable for both models.

This comparison gives some sense of the accuracy of the atomic rates, when the instrumental flux calibration ($\sim$ 25% for first order lines) is taken

into account. While uncertainties in the ionization and recombination rates are quite large, these data do not provide a test of the ionization balance models, since shifts in peak temperatures and relative ion population maxima may be easily accommodated by the fitting. In fact, the overall agreement of the observed lines with these models is only slightly worse than for lines taken for each ionization stage at its temperature of maximum ionization population. Thus, a factor of ±35% is the overall agreement of the line emissivities. While this level of agreement with theory is somewhat worse than one might expect from the collision strength uncertainties, we point out that many of the lines of Fe IX–XIV are sensitive to N_e. We also expect some spread in the forbidden-to-allowed line ratios due to omission of resonances in some of the collision strength calculations and the additional radiative terms. Furthermore, the observations may sample regions of different density along the line of sight. Of course, multiple densities would create a large spread, since the lines all have different nonlinear density dependences. While this model has been fit for all lines calculated at the best fitting density, $N_e = 10^{10}$ cm^{-3}, the spread in N_e derived from different line ratios is several orders of magnitude. Part of the scatter is undoubtedly due to measurement error as well. We include weak lines, and some of the lines may be blended. More detailed discussion of this analysis is found in Brickhouse *et al.* (1995).

Continuum emission has three major contributions. Bremsstrahlung produced by electrons which are accelerated in the electric fields of fully stripped H and He is a major continuum source throughout the high temperature region. Two-photon continua result from the decay of the H-like $2s\ ^2S$ level and the He-like $1s2s\ ^1S$ level. The sum of the photon energies equals the excitation energy of the level, and two-photon emission is an important contribution around 10^6 K. Radiative recombination produces a continuum spectrum which, as described above for the recombination rate coefficient, depends on the photoionization cross section. The current generation of model codes generally do not include the continua from recombination to excited levels. Under most circumstances this contribution is only a few percent. The calculations for all three sources of continuum emission should be accurate to about 10%.

3. Things That are Often Left Out

3.1. Mixed Collisional Ionization and Photoionization

Most model calculations are based on the assumption that photoionization is either dominant or completely negligible. Generally photoabsorption is taken to dominate the heating in photoionization models. Intermediate cases where both photoionization and collisional ionization contribute are not much more difficult to compute, but they represent an unpleasant increase in

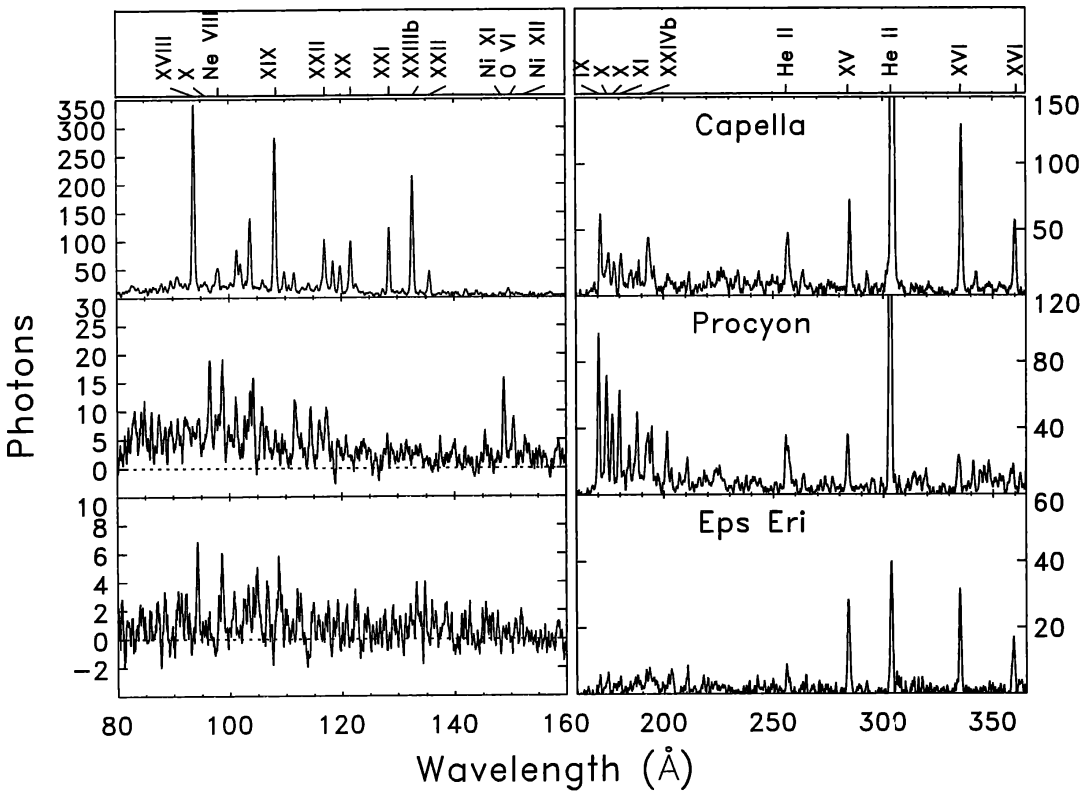

Fig. 1. *EUVE* spectra in the Short Wavelength (*left panel*) and Medium Wavelength (*right panel*) spectrometers for Capella (a binary system with G0 III and G8 III components), Procyon (F5 IV), and Epsilon Eridani (K2 V) (Courtesy of A. K. Dupree and G. J. Hanson). Species of Fe are marked by ionization stage. Fe XXIII λ132.85 is blended with Fe XX λ132.85; Fe XXIV λ192.02 is blended with Fe XII λ192.39, and may be difficult to resolve from Ca XVII λ192.86, and O V λλ192.75, 192.80, and 192.91.

the number of free parameters. Radiatively cooling gas, for instance behind a shock wave, presents a situation in which collisional ionization dominates the hotter regions, while photoionization becomes more important as the gas cools, so shock wave models always include both processes (*e.g.* Hartigan, Raymond and Hartmann 1987). Further complications arise if an external radiation source, such as an AGN or planetary nebula central star, is nearby (*e.g.* Contini and Viegas-Aldrovandi 1987). Any other interface between hot and cold plasma will present the same problem at some level. Examples include the helium lines from the Sun (*e.g.* Athay 1988), cooling flows in galaxy clusters (Voit, Donahue and Slavin 1994) or galactic halos (Sokolowski 1993), and thermal conduction boundaries (Slavin 1989).

3.2. Excitation by Ions

In a plasma with equal electron and ion temperatures, electrons move faster than protons by a factor of 43. Furthermore, the transitions most often

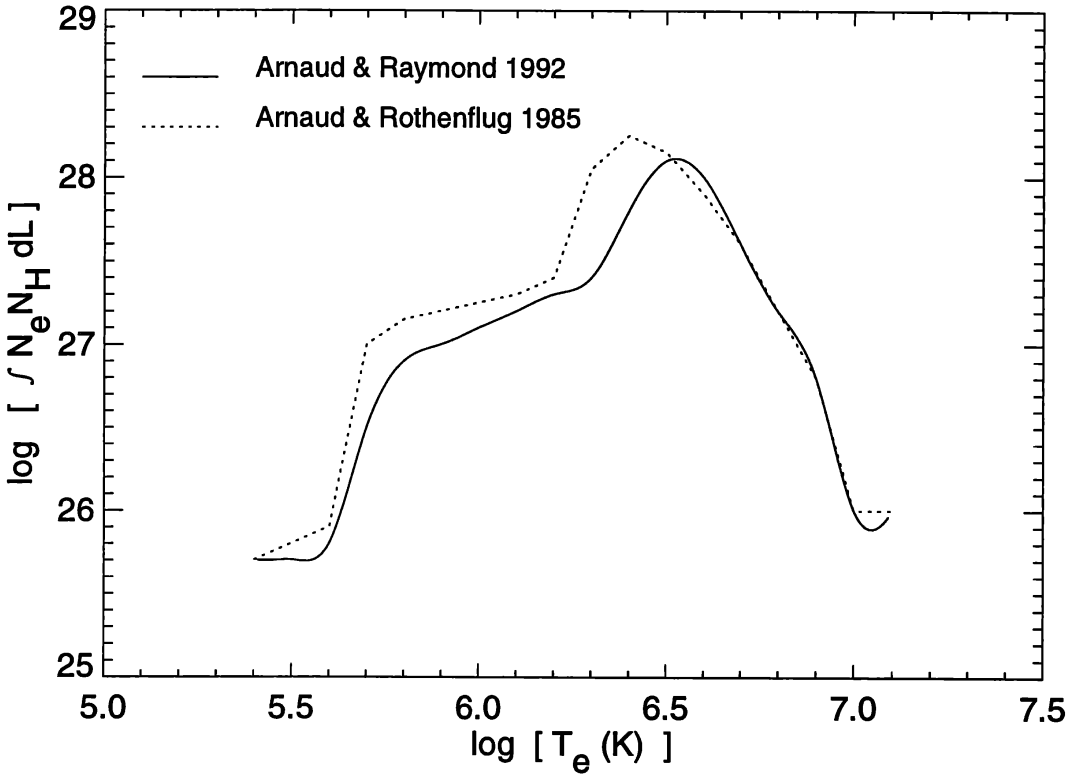

Fig. 2. Models of the emission measure distribution for the SERTS data, from Brickhouse *et al.* (1995). The solid line is the model for $N_e = 10^{10}$ cm^{-3}, assuming the ionization equilibrium of Arnaud and Raymond (1992). The dotted line is the model which assumes the ionization equilibrium of Arnaud and Rothenflug (1985).

observed have $\Delta E \sim kT$, and the cross sections at the ion speeds are small. However, there are cases where proton excitation is quite important. If $kT >> \Delta E$, the cross section for excitation by electrons drops at least as fast as ln E/E, and a proton appears to the ion much like a lower energy electron. Most of the cases which have been studied are fine structure transitions, such as infrared lines in the ISM (Bahcall and Wolf 1968), transitions which affect density diagnostics (*e.g.* those among $2s2p^3P$ levels in Be-like ions; Doyle *et al.* 1980) and the coronal lines [Fe X] λ6374 and [Fe XIV] λ5303 (Seaton 1964). Protons can initiate 2s-2p transitions in H-like ions, affecting the Lyα doublet ratio (Zygelman and Dalgarno 1987). Protons are also important for redistributing the populations of Rydberg levels, with consequences for radio recombination lines and for the density sensitivity of dielectronic recombination. Walling and Weisheit (1988) review these applications and provide formulae for semiclassical estimates of the cross sections.

Very fast shock waves also create conditions where proton excitation must be considered. Immediately behind the shock, low ionization species are immersed in extremely hot gas, so $kT_i >> \Delta E$ for many emission lines.

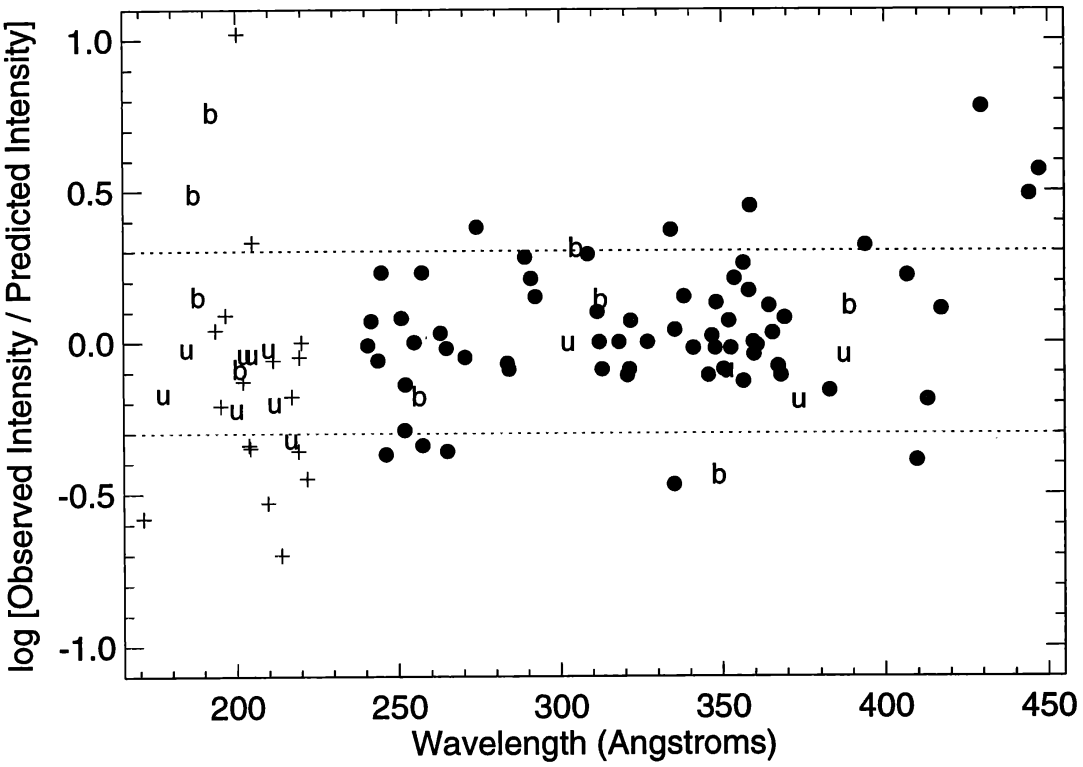

Fig. 3. Comparison of the observed and predicted intensities for the SERTS data and the solid line model in Fig. 2, shown versus wavelength. Filled circles = first order; plus signs = second order; b = blended (with a different element or ion); i = upper limit for the observation. Between the dotted lines, agreement is within a factor of 2.

Smith, Laming and Raymond (in preparation) find proton rates for excitation of Hα and for ionization of H° which are comparable to the electron rates for 1000 km/s shocks. Polarization of the Hα line is a possible diagnostic (Laming 1990b). Proton excitation of the UV lines of C IV, N V and O VI observed in the 2200 km/s shock of SN 1006 (Raymond, Blair and Long 1995) are larger than the electron rates, according to the formulae of Walling and Weisheit. The cross sections for excitation by ions generally scale as the square of the charge of the impinging ion, so helium nuclei can be significant in some cases.

3.3. Density Sensitive Ionization Balance

With the coronal approximation that all ions reside in their ground states, only the ionization and recombination rates from these states are of interest. However, Be-like and Mg-like ions have relatively low-lying metastable levels of high statistical weight ($g_m = 9$ *vs.* $g_g = 1$ for the ground state) so that most of the ions can be in the excited levels. Vernazza and Raymond (1979) attempted to incorporate those levels, but few of the relevant rates were available. A potentially interesting case, though we know of no specific

examples where it has been demonstrated to be important, is an ion whose ground state ionization potential is just above the photon energy of a strong line, but whose metastable level can be photoionized. The ^{3}P and ^{1}D levels of C I lie on either side of the Lyα photon energy, so one might expect a substantial decline in the C I emission of photodissociation regions or slow shock waves with increasing population of ^{1}D at high density.

Dielectronic recombination rate coefficients tend to decline at high densities as the highly excited intermediate states suffer collisional ionization (Burgess and Summers 1969). For charge states $z \sim 4$, this can reduce the rate by a factor of 2 at the densities $N_e \sim 10^{11}$ cm^{-3} found in solar active regions. The effect is strongest for ions whose dielectronic recombination goes by way of low photon energy transitions, such as Li-like ions (Summers 1976). The sensitivity scales roughly as $(N_e/Z^7)^{0.2}$. It is less likely to be important for highly charged ions or H-like, He-like or Ne-like ions, where the (relatively weak) dielectronic recombination requires $\Delta n \neq 0$ transitions. It is less important for low temperature dielectronic recombination (Storey 1981), which proceeds via much lower excited states. The dielectronic recombination is also sensitive to electric fields.

3.4. Electric Fields

The Stark effect can blend the higher levels of hydrogen into a quasicontinuum. A subtler effect is the enhancement of dielectronic recombination rates by Stark mixing of the ℓ levels of the doubly excited intermediate states (Reisenfeld 1992; Badnell *et al.* 1993; Story *et al.* 1995), but this effect is just beginning to be explored. Foukal, Little and Gilliam (1988) discuss the use of Stark broadening of the Paschen lines as an electric field diagnostic for the solar chromosphere. For both applications, the effects of plasma microfields (the random fields due to nearby ions) may be difficult to distinguish from macroscopic electric fields.

3.5. Resonant Scattering

Resonant scattering can affect observed line intensities in several ways. At optical depths ~ 1, the main effect is likely to be a geometrical redistribution of photons from optically thick directions to optically thin ones. Radiative shock waves in supernova remnants produce thin sheets of emitting gas, and the bright filaments seen in optical forbidden lines are tangencies of those sheets to the line of sight. While the forbidden lines have negligible optical depths, UV lines such as C IV λ1550 are strongly attenuated in the brightest filaments (Cornett *et al.* 1992). A similar effect has been invoked to explain Fe XVII line ratios in solar active regions (Schmelz, Saba, and Strong 1992). At somewhat greater optical depths, several scatterings can convert a photon to two or more lower energy photons. For an example, it takes on average eight scatterings to convert Lyβ to Hα plus a two photon

pair (at low density) or Hα and Lyα (at higher density). Similar conversions ought to be observable in the X-ray emission of hydrogenic and helium-like ions if optical depths are large. Finally, at large optical depths and high densities, collisional deexcitation becomes important as the lines begin to thermalize. Schrijver, van den Oord, and Mewe (1994) invoke optical depth effects to explain discrepancies between EUVE spectra of late-type stars and model calculations, but a complete calculation is likely to show drastic effects for some lines they did not consider. Schmitt, Drake, and Stern (1995a) suggest that contributions of weak lines to what Schrijver *et al.* identified as continuum could better explain the spectrum.

3.6. Radiative Excitation

Bowen (1935) investigated the resonance fluorescence process which converts a He II Ly α photon at 304 Å to O III photons near 3000 Å plus an EUV photon. Subsequent investigators have used improved atomic rates or extended the calculations to higher densities and line widths (Kallman and McCray 1980; Bhatia and Kastner 1990). Many other wavelength coincidences have been explored, including Ly β and O I (Athay and Judge 1995) and Ly α and H_2 (Jordan *et al.* 1977; Black and van Dishoeck 1987). Even an approximate coincidence can be important. Schmid (1989) showed that Raman scattering of the O VI doublet by hydrogen produces the $\lambda\lambda$ 6830, 7088 lines seen in symbiotic stars.

Continuum fluorescence can also be important. Ferguson *et al.* (1995) discuss the production of C III λ977 and other UV emission lines by continuum fluorescence in NGC 1068 as an alternative to shock heating. Continuum fluorescence of H_2 produces strong molecular features in photodissociation regions (Sternberg 1989).

Mason (1975) shows the effects of the photospheric radiation field on the emissivity calculations for a number of Fe and Ca optical forbidden lines in the solar corona. Calculations with updated atomic rate coefficients and photospheric radiation show that the excitation of [Fe X] λ6374 and [Fe XIV] λ5303 in low-density coronal hole regions may by dominated by this term (Esser *et al.* 1995).

3.7. Polarization and Emission Anisotropy

Particle velocity distributions, and therefore the radiation from the particles, are generally assumed to be isotropic. An exception is a directed particle beam producing X-rays in a solar flare. Laming (1990a) has shown that excitation by a beam produces different anisotropies in the Mg XII Ly α 1s-2p $^2P_{1/2}$ and 1s-2p $^2P_{3/2}$ lines. This can account for observed departures from the expected 1:2 ratio, depending upon the observer's location. Significant departure from isotropy also occurs behind a very fast shock wave. A neutral hydrogen atom can find itself immersed in very hot electrons and ions

moving at 3/4 the shock speed. Laming (1990b) has shown that this can produce polarization in Hα, which could be a useful diagnostic.

3.8. Non-Maxwellian Velocity Distributions

Direct measurements of the electrons in the only accessible astrophysical plasma - the solar wind - always seem to show non-Maxwellian distributions. Nevertheless, nearly all interpretations of astronomical spectra begin with the assumption that the distribution is Maxwellian. The most common departure from Maxwellian may be a non-thermal power law tail at high energies. This will naturally affect those processes with the highest thresholds, such as ionization or excitation of high-lying levels. Recombination and excitation of lines with $\Delta E \leq kT$ will be relatively unaffected. Owocki and Scudder (1983) explored the consequences of these distributions for the ionization state of the solar wind. Anderson, Raymond and van Ballegooijen (1995) considered the ionization balance and EUV emission line intensities for several velocity distributions in the velocity filtration picture of coronal heating (Scudder 1992). Laming (1990a) considered X-ray lines in solar flares. In general, a departure from Maxwellian which sets in only far above kT will have little effect on the dominant radiation processes, though it may affect the ionization state and energy balance (*e.g.* cosmic rays in a molecular cloud). If the departure sets in at $\sim$ 10 kT, the ionization state is drastically affected. It is unfortunately difficult to come up with a clean diagnostic for non-Maxwellian distributions. Line ratios of He-like ions are a recently suggested possibility (Gabriel *et al.* 1991).

3.9. Recombination to Excited Levels

In a collisionally ionized plasma, recombination to excited levels contributes little to emission line intensities. This comes about because ionizations must balance recombinations in equilibrium, and ionization rates are typically slower than the excitation rates of bright emission lines by at least an order of magnitude. Recombination to an excited level may be more competitive if the excitation from the ground state is forbidden or if the gas is overionized due to photoionization or extremely rapid cooling. Of course, if one is considering an important diagnostic line ratio, even a modest recombination contribution must be considered, as in He-like and H-like ions (Mewe and Gronenschild 1981). Other important cases include the X-ray emission in photoionized coronae in Low Mass X-ray Binaries (Liedahl *et al.* 1992), emission lines from gas strongly cooled by high concentrations of metals or dust (*e.g.* nova shells - Escalante and Dalgarno 1991), and specific lines pumped by dielectronic recombination at low temperatures (*e.g.* C III λ2297, N IV λ1718; Harrington, Lutz and Seaton 1981) or charge transfer (*e.g.* [O III] λ4363; Dalgarno and Sternberg 1987).

The most important recombination lines, for both energetic and diagnos-

tic purposes, may be the satellite lines formed during dielectronic recombination. These are caused by excitation of doubly excited levels lying below the threshold energy of the parent transition, and if the energy difference is substantial, the satellites can be relatively strong. They are resolvable from the parent transitions in highly charged ions, especially He-like and H-like ions (*e.g.* Beiersdorfer *et al.* 1993) and Fe XVII (Smith *et al.* 1985). These are included in the current generation of X-ray and UV model codes, and they are used as temperature and ionization state diagnostics in crystal spectrometer experiments on P78-1, SMM and YOHKOH (*e.g.* Doschek *et al.* 1990). Satellites to other iron lines in the 10 Å range may become important as better spectra and better rates for competing processes become available.

3.10. Ionization to Excited Levels

Ionization from an inner shell or inner subshell can leave an ion in an excited state and produce a photon. Feldman *et al.* (1992) have proposed that this might account for spectral anomalies in Fe XV. It requires severe departure from ionization equilibrium, again because ionization rates are generally slower than collisional excitation. It is not clear that such extremely rapid ionization would not create worse anomalies in the spectrum, and SERTS spectra suggest that the Fe XV intensities agree with equilibrium predictions after all (Brickhouse *et al.* 1995). Ionization to excited levels may be important in Fe XXV and some of its satellite lines, along with inner shell excitation.

3.11. Diffusion

Diffusion in a strong temperature gradient can modify both the ionization state at a given temperature and the relative elemental abundances. It has been invoked to explain the unexpected brightness of the He II lines in the Sun (Shine, Gerola, and Linsky 1975) and it may be important in enhancing the coronal abundances of low First Ionization Potential elements and in the energy balance in the upper chromosphere (Fontenla, Avrett and Loeser 1993). The effects of shifts in the ionization balance may be difficult to distinguish from time-dependent ionization (*e.g.* impulsive heating of the solar corona as in Raymond 1990) or non-Maxwellian distributions. The abundance variations observed, for example in the solar wind (*cf.* Meyer 1985), may provide a less ambiguous signature for some type of diffusion than emission line intensities.

4. Acknowledgements

This work was supported by NASA Grant NAG-528 to the Smithsonian Astrophysical Observatory.

References

Anderson, S. W., Raymond, J. C., and van Ballegooijen, A. 1995, submitted to *Ap. J.*
Arnaud, M. and Raymond, J. 1992, *Ap. J.*, **398**, 394.
Arnaud, M. and Rothenflug, R. 1985, *Astron. & Astrophys. Supp.*, L**60**, 425.
Athay, R. G. 1988, *Ap. J.*, **329**, 482.
Athay, R. G. and Judge, P. G. 1995, *Ap. J.*, **438**, 491.
Badnell, N. R., Pindzola, M. S., Dickson, W. J., Summers, H. P., Griffin, D. C. and Lang, J. 1993, *Ap.J. Lett.*, **407**, L91.
Bahcall, J. N. and Wolf, R. A. 1968, *Ap. J.*, **152**, 701.
Beiersdorfer, P., Phillips, T., Jacobs, V. L., Hill, K. W., Bitter, M., von Goeler, S., and Kahn, S. M. 1993, *Ap. J.*, **409**, 846.
Bhatia, A. K. and Kastner, S. O. 1990, *Ap. J.*, **352**, 772.
Bhatia, A. K. and Kastner, S. O. 1993, *JQSRT*, **49**, 609.
Black, J. H., and van Dishoeck, E. 1987, *Ap. J.*, **322**, 992.
Bowen, I. 1935, *Ap. J.*, **81**, 1.
Brickhouse, N. S. 1995, *IAU Coll. 152*, in press.
Brickhouse, N. S., Raymond, J. C. and Smith, B. W. 1995, *Ap. J. Supp.*, **97**, 551.
Burgess, A. and Summers, H. P. 1969, *Ap. J.*, **157**, 1007.
Callaway, J. 1994, *At. Data Nucl. Data Tables*, **57**, 9.
Contini, M. and Viegas-Aldrovandi, S. M. 1987, *Astron. & Astrophys.*, **185**, 31.
Cornett, R. H., *et al.* 1992, *Ap. J. Lett.*, **395**, L9.
Dalgarno, A. and Sternberg, A. 1982, *Ap. J. Lett.*, **257**, 87L.
Doschek, G. A., Fludra, A., Bentley, R. D., Lang, J., Phillips, K. J. H., and Watanabe, T. 1990, *Ap. J.*, **358**, 665.
Doyle, J. G., Kingston, A. E., and Reid, R. H. G. 1980, *Astron. & Astrophys.*, **90**, 97.
Drake, J. J., Laming, J. M., and Widing, K. G. 1995, *Ap. J.*, **443**, 393.
Dupree, A. K., Brickhouse, N. S., Doschek, G. A., Green, J. C., and Raymond, J. C. 1993, *Ap. J. Lett.*, **418**, L41.
Escalante, V. and Dalgarno, A. 1991, *Ap. J.*, **369**, 213.
Esser, R., Brickhouse, N. S., Habbal, S. R., Altrock, R. C., and Hudson, H. S. 1995, *J. Geophys. Res.*, in press.
Feldman, U., Laming, J. M., Mandelbaum, P., Goldstein, W. H., and Osterheld, A. 1992, *Ap. J.*, **398**, 692.
Ferguson, J. W., Ferland, G. J., and Pradhan, A. K. 1995, *Ap. J. Lett.*, **438**, L55.
Fontenla, J. M., Avrett, E. H., and Loeser, R. 1993, *Ap. J.*, **406**, 319.
Foukal, P., Little, R., and Gilliam, L. 1988, *Sol. Phys.*, **114**, 65.
Froese-Fischer, C. and Liu, B. 1986, *At. Data Nucl. Data Tables*, **34**, 261.
Gabriel, A. H., Bely-Dubau, F., Faucher, P., and Acton, L. W. 1991, *Ap. J.*, **378**, 438.
Gregory, D. C., Meyer, F. W., Müller, A., and DeFrance, P. 1986, *Phys. Rev. A*, **34**, 3657.
Gregory, D. C., Wang, L. J., Meyer, F. W., and Rinn, K. 1987, *Phys. Rev. A*, **35**, 3256.
Harrington, J. P., Lutz, J. H., and Seaton, M. J. 1981, *M.N.R.A.S.*, **195**, 21p.
Hartigan, P., Raymond, J. C. and Hartmann, L. H. 1987, *Ap. J.*, **316**, 323.
Heil, T. G., Kirby, K. and Dalgarno, A. 1983, *Phys. Rev. A*, **27**, 2826.
Huang, K.-N. 1986, *At. Data Nucl. Data Tables*, **34**, 1.
Jordan, C., Brueckner, G. E., Bartoe, J.-D. F., Sandlin, G. D., and van Hoosier, M. E. 1977, *Nature*, **270**, 326.
Kahn, S. M. and Liedahl, D. A. 1995, "X-Ray Spectroscopy of Cosmic Sources," in *Physics with Multiply Charged Ions*, NATO Advanced Study Institute Series, in press.
Kallman, T. R. and McCray, R. 1980, *Ap. J.*, **242**, 615.
Kastner, S. O., and Bhatia, A. K. 1990, *Ap. J.*, **362**, 745.
Kato, T., Masai, K., and Arnaud, M. 1991, *National Institute for Fusion Science Report*, ISSN 0915-6364.
Kwong, V. H. S., Fang, Z., Gibbons, T. T., Parkinson, W. H., and Smith, P. L. 1993, *Ap. J.*, **411**, 431.
Laming, J. M. 1990a, *Ap. J.*, **357**, 275.

Laming, J. M. 1990b, *Ap. J.*, **362**, 219.
Laming, J. M., Drake, J. J., and Widing, K. G. 1995, submitted *Ap. J.*
Lang, J., ed. 1994, 'Electron Excitation Data for Analysis of Spectral Line Radiation from Infrared to X-ray Wavelengths: Reviews and Recommendations,' *At. Data Nucl. Data Tables*, **57**.
Lang, J., Mason, H. E., and McWhirter, R. W. P. 1990, *Sol. Phys.*, **129**, 31.
Liedahl, D. A., Kahn, S. M., Osterheld, A. L., and Goldstein, W. H. 1990, *Ap. J. Lett.*, **350**, L37.
Liedahl, D. A., Kahn, S. M., Osterheld, A. L., and Goldstein, W. H. 1991, *Ap. J.*, **391**, 306.
Liedahl, D. A., Osterheld, A. L., and Goldstein, W. H. 1995, *Ap. J. Lett.*, **438**, L115.
Mason, H. E. 1975, *M.N.R.A.S.*, **170**, 651.
Mason, H. E. and Monsignori-Fossi, B. C. M. 1994, *A & A Rev.*, **6**, 123.
Mewe, R. 1991, *A & A Rev.*, **3**, 127.
Mewe, R. and Gronenschild, E. H. B. M. 1981, *Astron. & Astrophys.*, **45**, 11.
Mewe, R., Kaastra, J. S., Schrijver, C. J., van den Oord, G. H. J., and Alkemade, F. J. M. 1995, *Astron. & Astrophys.*, **296**, 477.
Meyer, J. P. 1985, *Ap. J. Supp.*, **57**, 173.
Osterbrock, D. E. 1974, "Astrophysics of Gaseous Nebulae," W. H. Freeman and Co.: San Francisco.
Opacity Project Team, 1995, "The Opacity Project," Vol. 1, Institute of Physics Publishing: Bristol.
Owocki, S. P. and Scudder, J. D. 1983, *Ap. J.*, **270**, 758.
Pradhan, A. K. and Gallagher, J. W. 1992, *At. Data Nucl. Data Tables*, **52**, 227.
Pradhan, A. K. and Peng, J. 1995, "Atomic Data for the Analysis of Emission Lines," in *Proceedings of the Space Telescope Science Institute Symposium in Honor of the 70th Birthdays of D. E. Osterbrock and M. J. Seaton.*
Raymond, J. C. 1988, in "Hot Thin Plasmas in Astrophysics," R. Pallavicini, ed., Kluwer: Dordrecht, p. 1.
Raymond, J. C. 1990, *Ap. J.*, **365**, 387.
Raymond, J. C., Blair, W. P., and Long, K. S. 1995, *BAAS*, **27**, 854.
Reisenfeld, D.B. 1992, *Ap. J.*, **398**, 386.
Schmelz, J. T., Saba, J. L. R., and Strong, K. T. 1992, *Ap. J.*, **398**, 115.
Schmid, H. M. 1989, *Astron. & Astrophys.*, **211**, L31.
Schmitt, J. H. M. M., Drake, J. J., and Stern, R. A. 1995a, *IAU Coll. 152* abstracts.
Schmitt, J. H. M. M., Drake, J. J., Stern, R. A., Haisch, B. M. 1995b, submitted *Ap. J.*
Schrijver, C. J., van den Oord, G. H. J., and Mewe, R. 1994, *Astron. & Astrophys.*, **289**, L23.
Scudder, J. D. 1992, *Ap. J.*, **398**, 319.
Seaton, M. J. 1964, *M.N.R.A.S.*, **127**, 191.
Shine, R., Gerola, H., and Linsky, J. L. 1975, *Ap. J. Lett.*, **202**, L101.
Slavin, J. D. 1989, *Ap. J.*, **346**, 718.
Smith, B. W., Raymond, J. C., Mann, J., and Cowan, R. D. 1985, *Ap. J.*, **298**, 898.
Sobelman, I. I., Vainshtein, L. A., and Yukov, E. A. 1981, "Excitation of Atoms and Broadening of Spectral Lines," Springer-Verlag: New York.
Sokolowski, J. K. 1992, Ph.D. Thesis, Rice University.
Sternberg, A. 1989, *Ap. J.*, **347**, 863.
Storey, P. J. 1981, *M.N.R.A.S.*, **195**, 27P.
Story, J. G., Lyons, B. J., and Gallagher, T. F. 1995, *Phys. Rev. A*, **51**, 2156.
Summers, H. P. 1974, *M.N.R.A.S.*, **169**, 663.
Thomas, R. J. and Neupert, W. M. 1994, *Ap. J. Supp.*, **91**, 461.
Vernazza, J.E. and Raymond, J. C. 1979, *Ap. J. Lett.*, **228**, L89.
Verner, D. A., Yakovlev, D. G., Band, I. M., and Trzhaskovskaya, M. B. 1993, *At. Data Nucl. Data Tables*, **55**, 223.
Verner, D. A. and Yakovlev, D. G. 1995, *Astron. & Astrophys. Supp.*, **109**, 125.

Voit, G. M., Donahue, M., and Slavin, J. D. 1994, *Ap. J. Supp.*, **95**, 87.
Walling, R.S. and Weisheit, J.C., 1988, *Physics Reports*, **162**, 1.
Zygelman, B. and Dalgarno, A. 1987, *Phys. Rev. A*, **35**, 4085.